scientific reports

Check for updates

OPEN

Longitudinal growth of the *Saccharina* kelp embryo depends on actin filaments that control the formation of a corset-like structure composed of alginate

Samuel Boscq[1,4], Ioannis Theodorou[1,2,4], Roman Milstein[1], Aude Le Bail[1], Sabine Chenivesse[1], Bernard Billoud[1,3] & Bénédicte Charrier[1,3]✉

The initiation of embryogenesis in the kelp *Saccharina latissima* is accompanied by significant anisotropy in cell shape. Using monoclonal antibodies, we show that this anisotropy coincides with a spatio-temporal pattern of accumulation of alginates in the cell wall of the zygote and embryo. Alginates rich in guluronates as well as sulphated fucans show a homogeneous distribution in the embryo throughout Phase I of embryogenesis, but mannuronate alginates accumulate mainly on the sides of the zygote and embryo, disappearing as the embryo enlarges at the start of Phase II. This pattern depends on the presence of cortical actin filaments. In contrast, within the embryo lamina, the alginate composition of the walls newly formed by cytokinesis is not affected by the depolymerisation of actin filaments. Thus, in addition to revealing the existence of a mannuronate-rich alginate corset-like structure that may restrict the enlargement of the zygote and the embryo, thereby promoting the formation of the apico-basal growth axis, we demonstrate stage- and cytoskeleton-dependent differences in cell wall deposition in *Saccharina* embryos.

Brown algae are multicellular organisms that are characterised by a high diversity of body shapes[1], ranging from microscopic uniseriate filaments (e.g. *Ectocarpus* spp[2,3]) to metres-long, thick blades (e.g. *Saccharina* spp[4]). This great diversity of body shapes is due to the diversity of growth patterns. Brown algae feature different strategies for the spatio-temporal coordination of growth rate, growth location and growth direction in the three spatial axes, making them a model evolutionary group to investigate the various mechanisms underlying the acquisition of body axes and shape diversity in multicellular organisms.

The study of the embryogenesis of brown algae has led to the identification of several cellular and molecular factors inducing symmetry breaking. For example, the extremely polarised growth of the *Ectocarpus* filament depends on the Rho-GTPase pathway involved in the organisation of actin filaments[5], but no major triggering environmental factor has been identified. In contrast, the embryo of Fucales (e.g. *Fucus*, *Silvetia*, *Pelvetia* spp) polarises and germinates away from and parallel to the light source[6]. The fertilisation site of the male gamete on the surface of the *Fucus* egg is also a positional cue triggering polarisation of the zygote[7]. This polarisation becomes apparent with the formation of a patch of actin filaments and the secretion of sulphated polysaccharides from the cell wall at the point where the rhizoid emerges[8,9]. To date, no studies of this type have yet been carried out on kelps (e.g. *Saccharina*). However, these brown algae have an interesting morphological feature. Unlike *Ectocarpus*, whose body plane is limited to the single axis of the uniserial filament (1D), and *Fucus*, whose embryo acquires its 3D architecture according to the sequence of the first three cell divisions of the thallus cell of the early embryo[10], in the Laminariales, embryogenesis is characterised by phases (or plateaus), during which growth is limited to first one axis (1D growth), then two axes (2D growth) before finally establishing the three perpendicular body axes making a 3D body[11,12]. This feature makes them particularly amenable to the investigation of the factors controlling the establishment of body planes during embryogenesis.

[1]Morphogenesis of Macro Algae, UMR8227, CNRS - Sorbonne University, Station Biologique de Roscoff, Place Georges Teissier, Roscoff 29680, France. [2]Plant Sciences Department, Faculty of Biosciences, Norwegian University of Life Sciences, Ås, Norway. [3]Present address: Morphogenesis of Brown Algae, Institut de Génomique fonctionnelle de Lyon (IGFL), UMR5242, ENS-Lyon, CNRS, INRAE, UCBL, 32-34 avenue Tony Garnier, Lyon 69007, France. [4]Co-first authors: Samuel Boscq and Ioannis Theodorou. ✉email: benedicte.charrier@cnrs.fr

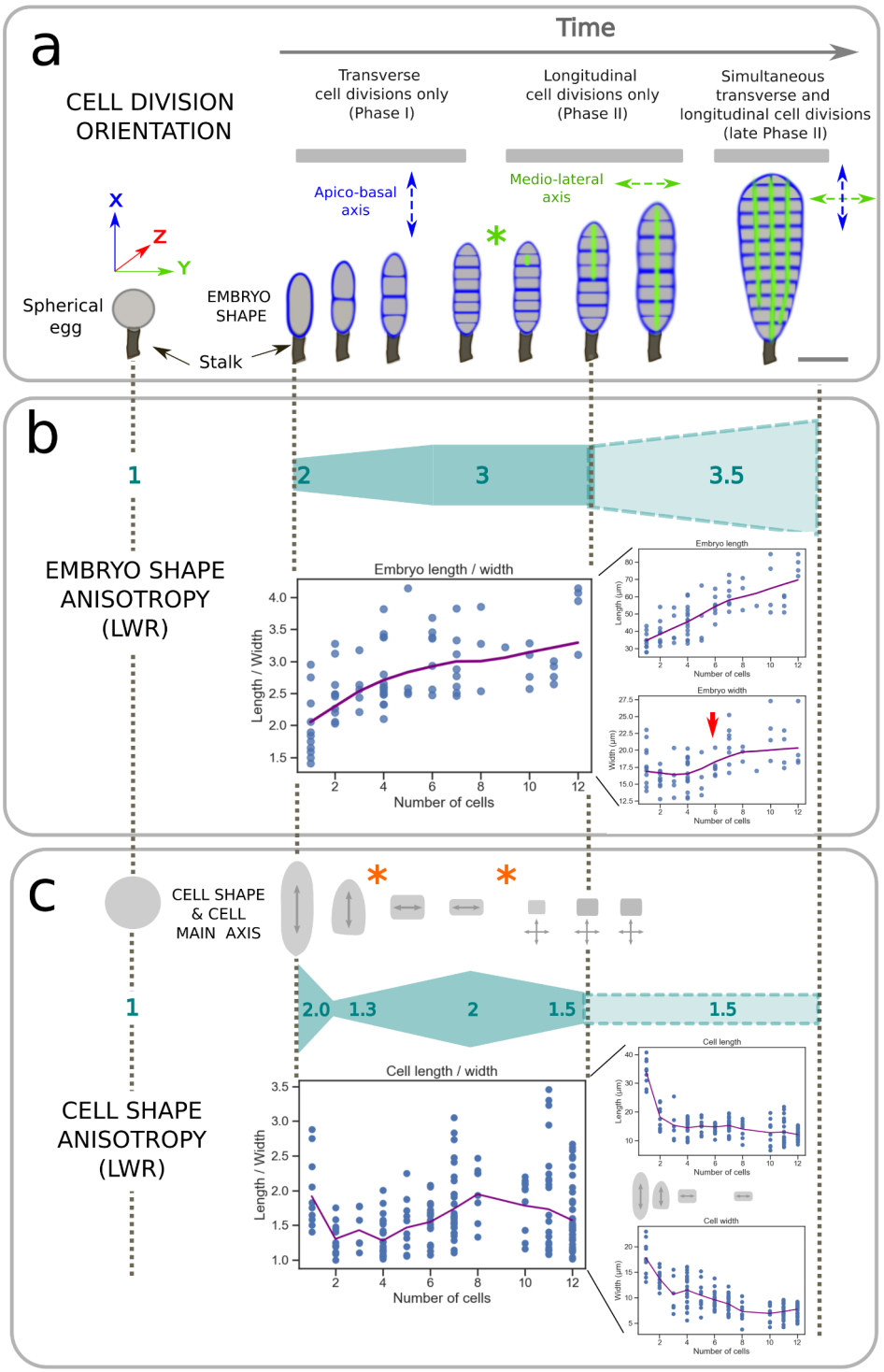

We have recently described in detail these three morphological steps in the embryogenesis of *Saccharina*, particularly the transition from 2D to 3D growth, which, in this species, is accompanied by cell differentiation[13]. After fertilisation, the zygote first elongates along an axis parallel to the maternal stalk, which is the remnant envelope (cell wall) of the oogonium that sits on the gametophyte filament (Fig. 1a, left). The zygote thereby acquires its first body axis, which is the longitudinal axis (X-axis). Then, the second step corresponds to the maintenance of this initial body axis with a series of three cell division rounds in a plane perpendicular to the longitudinal axis of the zygote (each cell divides, almost synchronously) resulting in the formation of a stack of 8 cuboid cells (2^3 cells, Fig. 1, left, Phase I;[13]). At this stage, the orientation of the next cell division tilts by 90°, which results in the formation of a second body axis, i.e. the medio-lateral axis (Y-axis) and the initiation of Phase II as defined in[13] (Fig. 1, middle). After a series of alternations of transverse and longitudinal cell divisions, resulting in a monolayered lamina of ~ 1000 cells (Fig. 1a, right), the cell division orientation again tilts by 90° in

◀**Fig. 1**. Anisotropy in the *Saccharina latissima* embryo. Development of the *S. latissima* embryo over time. (**a**) Schematics of the embryos from the zygote stage to Phase II (after cells divided longitudinally). Upon fertilisation, the zygote elongates (blue outline), establishing the first growth axis parallel to the maternal stalk (black peduncle) (left-hand side). Then, the early-stage embryo continues to develop longitudinally through transverse cell divisions (blue lines), forming the apico-basal axis (Phase I). Phase II starts with the first longitudinal cell division (green line), generally in the most apical region of the embryo (middle, top of the embryo). All cells eventually divide longitudinally, but this division is delayed in the basal cell. The green asterisk illustrates the change in cell division orientation, i.e. from transverse to longitudinal. Scale bar = 50 µm. (**b**) Anisotropy in the morphology of the embryos. (Top) Schematised gradient of shape anisotropy (expressed as the Length-to-Width ratio LWR, unitless), along the development of the embryo, from the 1-cell stage (eggs, defined by LWR in [1.0;1.2] and zygotes with LWR = 2, shown as blue numbers), to the 12-cell stage (early Phase II). (Bottom) Graphics plotting the embryo shape anisotropy value (centre), as well as the embryo length (µm; top right) and the embryo width (µm; bottom right) over time (expressed as the number of cells of the embryo). The purple lines show the mean value, smoothed using the lowess function. The red arrow shows the increase in width of the embryo. (**c**) Shape anisotropy of the embryo cells. (Top) Cell shape outlines at each developmental stage (grey shapes) with the orientation of their main growth axis indicated (double grey arrows inside each cell; perpendicular arrows indicate that both orientations are possible). Only recently divided cells are shown. The orange asterisks indicate changes in orientation of the main cell axis. (Middle) Schematised gradient of cell shape anisotropy along the development of the embryo. Cell LWR values are indicated as blue numbers. (Bottom) Graphics plotting the cell shape anisotropy value, as well as the cell length (µm; top right) and the cell width (µm; bottom right) over time (expressed as the number of cells of the embryo). The purple line shows the mean value. Note that cell length is defined as the longest cell dimension and cell width as the shortest, irrespective of the orientation of the cell in the embryo.

the third spatial axis (i.e. Z-axis), leading to lamina thickening (polystromatisation)– while continuing to grow in the other two axes – and cell differentiation.

This exceptional series of ordered shifts, from 1D to 2D and then 3D growth at the level of the embryo, suggests that important positional cues are part of a regulation mechanism that promotes or suppresses the shifts in cell division orientations at one given stage. The maintenance of a given orientation of cell division over several division cycles is also an interesting feature, especially as in some cases it involves the formation of cells with a very high level of shape anisotropy, which, according to the canonical rules of cell division[14], requires specific constraints.

We have recently shown that the maintenance of the longitudinal axis depends on the contact of the embryo with the maternal stalk, which is the compartment from which the egg was extruded[15]. This study suggested that a signal, most likely chemical, emanates from the maternal stalk (remnant oogonium), reaching and diffusing across the basal cell[16] and exerting acropetal control of longitudinal cell divisions. This control seems to be most prominent at Phase I during which the embryo reaches 8 cells, because severing the stalk before that stage results in embryos that grow isotropically.

At this stage of understanding the mechanisms controlling body axis establishment during the embryogenesis of *S. latissima*, we aimed first to precisely characterise the levels of anisotropy experienced by the embryo during its development, and second, to identify the molecular factors that might underlie this anisotropy.

Results

Embryogenesis in *Saccharina latissima* is accompanied by a complex pattern of embryo and cell morphological anisotropy

The sequential acquisition of the three body axes, characterised by plateaus during which the alga grows in certain axes, separated by abrupt transitions during which the alga starts growing in a new axis, involves 90° changes in the orientation of cell division at each transition. To determine whether the orientations of cell division depend on embryo and/or cell shape, we monitored several embryos during Phase I and early Phase II, and studied the relationship between emergence and maintenance of body axes in the embryo, and the degree of body and cell shape anisotropy.

After fertilisation, the spherical egg (length-to-width ratio (LWR) = 1) elongates. This is the first anisotropy step of embryogenesis during which the embryo acquires it first body axis, which is the longitudinal apico-basal axis (Fig. 1a, left). As the embryo continues to grow, its shape becomes increasingly anisotropic (Fig. 1a, b; Supplementary Table S1a) up to the 8-cell stage, where its LWR reaches 3.0, before dropping back to 2.5 at the 160-cell stage (Supplementary Fig. S1a). Detailed analysis of embryo length and width showed that, during Phase I, the embryo grew 36.2 µm in length while its width increased by only 2.7 µm (Fig. 1b, graphic middle right); calculated from the 1-cell to the 8-cell stages; Supplementary Table S1a). Thus, the anisotropy of growth of the embryo is due to a limitation of growth in width, i.e. along the medio-lateral axis (Y). Interestingly, width was stable at 17.6 µm until the ~ 6-cell stage, when it started to increase (Fig. 1b, graphic bottom right, red arrow). This corresponds to the transition from Phase I to Phase II, defined by the change in cell division orientation from exclusively transverse to exclusively longitudinal (Fig. 1a, centre), until it alternates between transverse and longitudinal (Fig. 1a, right). Therefore, the 90° tilt in cell division orientation coincides with an increase in embryo width.

The anisotropy dynamics of individual cells making the embryo differ from that of the whole embryo. Once the zygote has divided, cells and the embryo have different trajectories of shape variation. As a whole, the anisotropy of the embryo continues to increase from the zygote to the 7–8 cell stage (Fig. 1b, centre), but at the

individual cell level, anisotropy varies more often (Fig. 1c; Supplementary Table S1B): the zygotic cell had the highest degree of anisotropy (LWR ≈ 2), after its elongation upon fertilisation. Then, due to the first embryonic cell division, cell LWR drops to 1.3, meaning that the first two embryonic cells are almost isotropic (Fig. 1c, middle). The second and third rounds of transverse cell division increased the degree of anisotropy again to ≈ 2 (8-cell stage). This increase was due to the maintenance of transverse cell divisions with very little cell growth. As a result, not only does shape anisotropy increase — cells became much thinner in width (from 13.7 to 7.3 µm; Fig. 1c, graphic bottom right), while their length was almost unchanged (from 18.2 to 14.0 µm; Fig. 1c, graphic middle right) —, but also the cell axis tilts by 90° : initially aligned with the apico-basal axis of the zygote and the 2-cell stage embryo, the cell axis aligned with the medio-lateral axis at the 4-cell stage onwards (first red asterisk in Fig. 1c, top). During the transitions from Phase I to Phase II, cell shape anisotropy began to decrease again, to LWR 1.5, which then remained stable throughout Phase II (Supplementary Fig. S1c). In addition, at this stage, the cell axis alternated at almost each cell division (second red asterisk).

Therefore, embryonic Phase I was characterised by two main events of morphological anisotropy: first, the elongation of the zygote, resulting from the retraction of the egg's flanks after fertilisation, and second, recurrent transverse cell divisions that take place with virtually no cell growth and in the same orientation as the cell main axis, resulting in highly anisotropic cell shapes. The fact that this maximal cell shape anisotropy was observed just before cells tilt their cell division planes suggests that high cell shape anisotropy would contribute to trigger the change in cell division orientation. Thus, to "bend the bow" (i.e. making cells highly anisotropic before tilting the cell division plane), there must be mechanisms that force cell divisions to be parallel to the longest cell axis.

Alginate and fucan cell wall polysaccharides display different spatio-temporal patterns during embryogenesis in *Saccharina latissima*

To identify the cellular or molecular factors involved in the control of the complex anisotropy patterns characteristic of the *Saccharina* embryo, we first looked for potential molecular markers in the cell wall. The cell wall of brown algae is composed of mainly alginates and fucans that embed a small proportion of cellulose microfibrils[17–19]. Chains of alginates are composed of different epimers, namely mannuronan acids (M) and guluronan acids (G) usually mixed within the chains as M-M, M-G or G-G blocks, which can be distinguished by the BAM6-11 series of monoclonal antibodies[20]. Fucans can be present with different levels of sulphation, which can be targeted by the BAM1-4 series of antibodies[21]. We took advantage of the specificity of these antibodies to try to identify molecular markers of anisotropy in the *Saccharina* embryo.

We observed that recently fertilised eggs are enveloped by a homogeneous layer of mannuronate-rich alginates (i.e. rich in M-M blocks, labelled with monoclonal antibody BAM6) (Supplementary Fig. S2a, left). In contrast, in zygotes, they appeared to be present only along the flanks of the cell, with the apex and the base of the zygote being devoid of any signal (Fig. 2a). This corset-like structure made of M-M-rich alginates surrounding the zygote persisted up to the 6–8 cell stage (Fig. 2b–g). Very interestingly, this corset-like structure disappeared as the embryo switched to Phase II, when transverse cell walls were labelled simultaneously (Fig. 2h–k). This pattern in which only the cross walls (both transversal and longitudinal), and not the external walls (corset-like structure) were labelled, persisted in Phase II embryos (Fig. 2l–o) and beyond (Supplementary Fig. S2a, right). It is noteworthy that M-M-rich alginates accumulated in the innermost layer of the cell wall of the cells within the embryo, so that two distinct cell walls were observed at each boundary between two cells, separated by a layer of cellulose microfibrils (Fig. 2p). Therefore, M-M rich alginates appear to be present in the most recent cell wall layers, which is in agreement with reports in embryos of Fucales (*Silvetia*)[22].

In summary, M-M-rich alginates were found in all cells, except in the apex and base of the embryos. From our observations, in the early stages, S*accharina* embryos do not grow apically and even less basally; instead growth is diffuse, carried out by all the cells. Therefore, the absence of M-M-rich alginates in the apex and base of the embryo raises questions about their role in *Saccharina* embryogenesis.

The BAM7 antibody, which labels M-G-rich alginates[20], did not display the same spatio-temporal pattern as the BAM6 antibody (Supplementary Fig. S2b). In contrast to M-M-rich alginates, M-G-rich alginates were homogeneously distributed in fertilised eggs and zygotes, not only along the flanks, but also at the apex and the base of the embryo. In addition, right after the zygote stage, these alginates were no longer detected in the external cell wall and accumulated in the cross walls only (Supplementary Fig. S2b). At the sub-cellular level, M-G-rich alginates appeared to be detected in the innermost layer, like M-M-rich alginates (Supplementary Fig. S2b).

Guluronate-guluronate (G-G)-rich alginates, labelled by monoclonal antibody BAM10[20] were detected at the surface of embryos from the egg stage to mature Phase II (Supplementary Fig. S2c, right). In comparison, these polysaccharides were barely detected in cross walls, where the signal was much weaker than that of Calcofluor white, which binds to cellulose microfibrils (Supplementary Fig. S2c, blue channel).

A similar pattern was found for fucans, which are abundant components of cell walls in most brown algae[17,23]. Using the monoclonal antibody BAM4[21], we observed that sulphated fucans uniformly envelop the surface of fertilised eggs, zygotes and embryos until late Phase II at least (Supplementary Fig. S2d), but not in the cross walls of Phase II embryos (Supplementary Fig. S2d). Interestingly, like G-G-rich alginates in the envelope of fertilised eggs and zygotes (Supplementary Fig. S2c), sulphated fucans were detected more externally than cellulose (in e.g. zygote in Supplementary Fig. S2c and Phase I and II embryos in Supplementary Fig. S2d).

In contrast to alginates and fucans that are present in specific locations during the development of *Saccharina* embryo, cellulose labelled with Calcofluor white appeared to be distributed homogeneously in the external cell wall and in all the cross walls from the egg to the Phase II stages (Supplementary Fig. S2a–d).

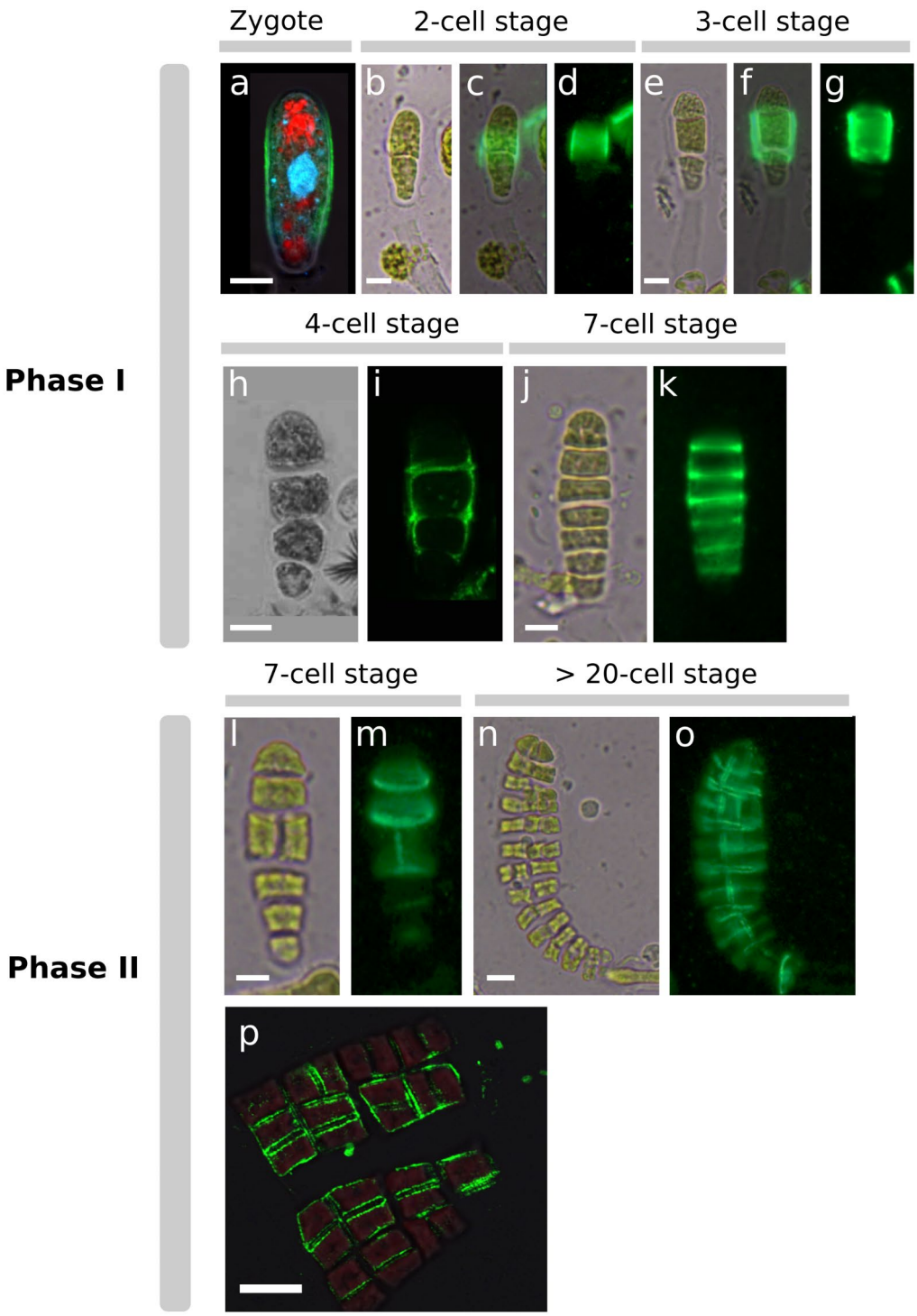

Fig. 2. Detection of mannuronate-rich alginates during the development of *Saccharina* embryos. Zygote and embryos up to the > 20-cell stages were labelled with the monoclonal antibody BAM6, which is specific to mannuronate-rich alginates. (**a**) zygote, (**b**–**d**) 2-cell stage embryo, (**e**–**g**) 3-cell stage embryo, (**h**–**i**) 4-cell stage embryo, (**j**–**k**) 7-cell stage embryo, (**l**–**m**): 7-cell stage embryo having divided longitudinally (formally, a Phase II embryo), (n-p): Phase II embryos (with transverse and longitudinal cell divisions). (**b**, **e**, **h**, **j**, **l**, **n**): bright field images. (**d**, **g**, **k**, **m**, **o**): epifluorescence of FITC-BAM6 antibody (green signal). (**c**, **f**) merge. (**a**, **h**, **i**, **p**) confocal images. (**p**) close-up of a blade of a Phase II embryo showing mannuronate-rich alginates in the innermost cell wall of each cell (green: FITC; red: chloroplast autofluorescence; blue: Calcofluor; cyan: DAPI). Scale bars = 10 µm.

Actin filaments are localised cortically in phase I and Phase II embryos

In some brown algae belonging to the orders Fucales and Sphacelariales, the accumulation of cell wall components depends on the organisation of actin filaments (AFs)[9,24–27]. To assess the role of AFs in the formation of the cell wall during *Saccharina* embryogenesis, and more specifically in the establishment of its morphological and molecular anisotropy, we labelled AF-fixed embryos with rhodamine-phalloidin or Alexa Fluor™ 488 phalloidin. In zygotes, we observed a network of cortical AFs throughout newly formed zygotes (Fig. 3a, b, grey arrows). This accumulation in the cell cortex was maintained in Phase I embryos (Fig. 3c), and even more clearly in Phase II, where all the innermost sides of the cuboid cells that characterise Phase II were homogeneously labelled (Fig. 3d, e). The cortical localisation of AFs is not specific to the *Saccharina* embryo, having been observed in other brown algae, particularly when cells are in interphase[28]. Interestingly, a weaker signal was observed at the lateral sides of the embryo blade, along the walls on the outward-facing edges of the embryo (Fig. 3d, e, white asterisks). This distinct pattern suggests that the role of AFs in the cells of the lamina differs between the inner edges (cross walls) shared by neighbouring cells and the outer edges (surface walls) where cell faces are in direct contact with the seawater. This interpretation is supported by the different orientations of AFs in Phase II embryos (Supplementary Fig. S3), which are all aligned along the Z-axis perpendicularly to the embryo apico-basal axis (Supplementary Fig. S3a, c); orientation angle = 77.69° ± 10.43 relative to the surface of the lamina (Supplementary Fig. S3d, left and Supplementary Fig. S3e), except when they are close to the front and back surfaces of the embryo, along the cell faces in contact with seawater (Supplementary Fig. S3b; angle = 50.37° ± 26.41; Supplementary Fig. S3d, right and Supplementary Fig. S3e). This specific orientation of AFs perpendicular to the lamina surface is accompanied by a greater abundance of AFs compared with the surface AFs (Supplementary Table S2, Two-sided Mann-Whitney (U-test) p-value = 0.000751). This highly ordered organisation may be involved in the differential organisation of the cell wall.

Actin filaments control cell shape

To further characterise the processes that control the specific organisation of the cell wall in *Saccharina*, we treated *Saccharina* embryos with latrunculin B (LatB), a drug that binds actin monomers and blocks their polymerisation into AFs[29]. Embryos were treated for 7 days with 50, 100, 500 or 1000 nM LatB in seawater. Control embryos immersed in 1% DMSO grew with no malformation (Fig. 4a), but LatB-treated embryos showed reduced growth and displayed abnormal morphologies (Fig. 4b–i). These morphological responses were observed for LatB concentrations as low as 50 nM (Fig. 4b, c), for which fertilised eggs and zygotes grew into cells larger than the control, and with irregular shapes. The extent of the impact of LatB on the morphology of the embryo increased with LatB concentrations from 100 nM up to 1 µM (Fig. 4d–i). Zygotes swelled and grew asymmetrically, generating protuberances in all three spatial directions (e.g. Figure 4b), or a pair of spherical cells along the medio-lateral direction (Fig. 4g). Some returned to an isotropic shape, losing their elongated shape and apico-basal axis (Fig. 4e, i). These abnormal morphologies indicate that AFs are involved in maintaining the elongated shape of the zygote, and in controlling the orientation of divisions during Phase I, when it occurs in these conditions (indicated by red asterisks in Fig. 4c, f,g, i). However, AFs are also necessary for cytokinesis[28] and LatB treatment usually inhibits cell division. The effect of LatB on the orientation of cell division diminished once the first transverse division occurred, and only cell shape was affected (Fig. 4d, h).

Actin filaments control the spatio-temporal pattern of mannuronate-rich alginates during *Saccharina* embryogenesis Phase I and Phase II

To assess whether AFs are functionally related to the composition of the cell wall, and specifically involved in the anisotropic pattern of M-M-rich alginates along the flanks of the embryos, we repeated the labelling experiments of alginates and fucans on fertilised eggs, zygotes and embryos in the presence of LatB. When treated with 1 µM LatB for 1 week, fertilised eggs, zygotes and embryos showed reduced anisotropy, as observed in Fig. 4. In addition, M-M-rich alginates accumulated in the apex of zygotes in addition to the flanks (Fig. 5a–f), unlike control embryos (Fig. 2 and text above). Labelled M-M-rich alginates in the tip of the embryos persisted to the 7-cell stage (Fig. 5g–j): the first apical half of the embryos was homogeneously labelled in addition to the transverse cell walls. Therefore, in response to LatB, the corset-like structure of M-M-rich alginates, limited to the flanks of the control embryos, is transformed into a "sock" covering both the flanks and the apex. In Phase II embryos, M-M-rich alginates were observed on the boundary of the blade (Fig. 5m–v; Supplementary Fig. S4a). This pattern contrasts with the pattern observed in control embryos in which the blade boundary was devoid of M-M-rich alginates. The labelling of transverse cell walls in response to LatB remained unchanged (Fig. 5r, t, v).

In summary, LatB-mediated depolymerisation of AFs resulted in a ubiquitous accumulation of the BAM6 epitope in the periphery (outer cell wall) of the egg, zygote and embryos and in the transverse cell walls within the lamina. This maintenance of an ubiquitous accumulation of M-M rich alginates from the egg stage until the end of Phase II, is in contrast to the change observed between Phase I and Phase II in control embryos.

Thus, AFs play a role in the control of mannuronate-rich alginate accumulation or organisation in the external cell wall that grows and thickens as of the zygote stage, but not in the transverse and longitudinal cross walls that are formed by cytokinesis.

Remarkably, this regulation of the spatio-temporal accumulation pattern is highly specific to M-M-rich alginates, because no such modification was observed in the presence LatB when using BAM7, and BAM10 antibodies (compare Supplementary Fig. S4b–d with Supplementary Fig. S2b–d). However, it is noteworthy that the alginate signal was less well defined in the presence of LatB than in control growth conditions. Uneven patches of FITC were observed when using BAM6 and BAM7 (Supplementary Fig. S4a, b), suggesting a major misregulation of M-M-rich and M-G-rich alginate accumulation in these embryos. Altogether, this result supports that the localisation of M-M-rich alginates, and to a lesser extent M-G-rich alginates, is impaired in LatB-treated *Saccharina* embryos.

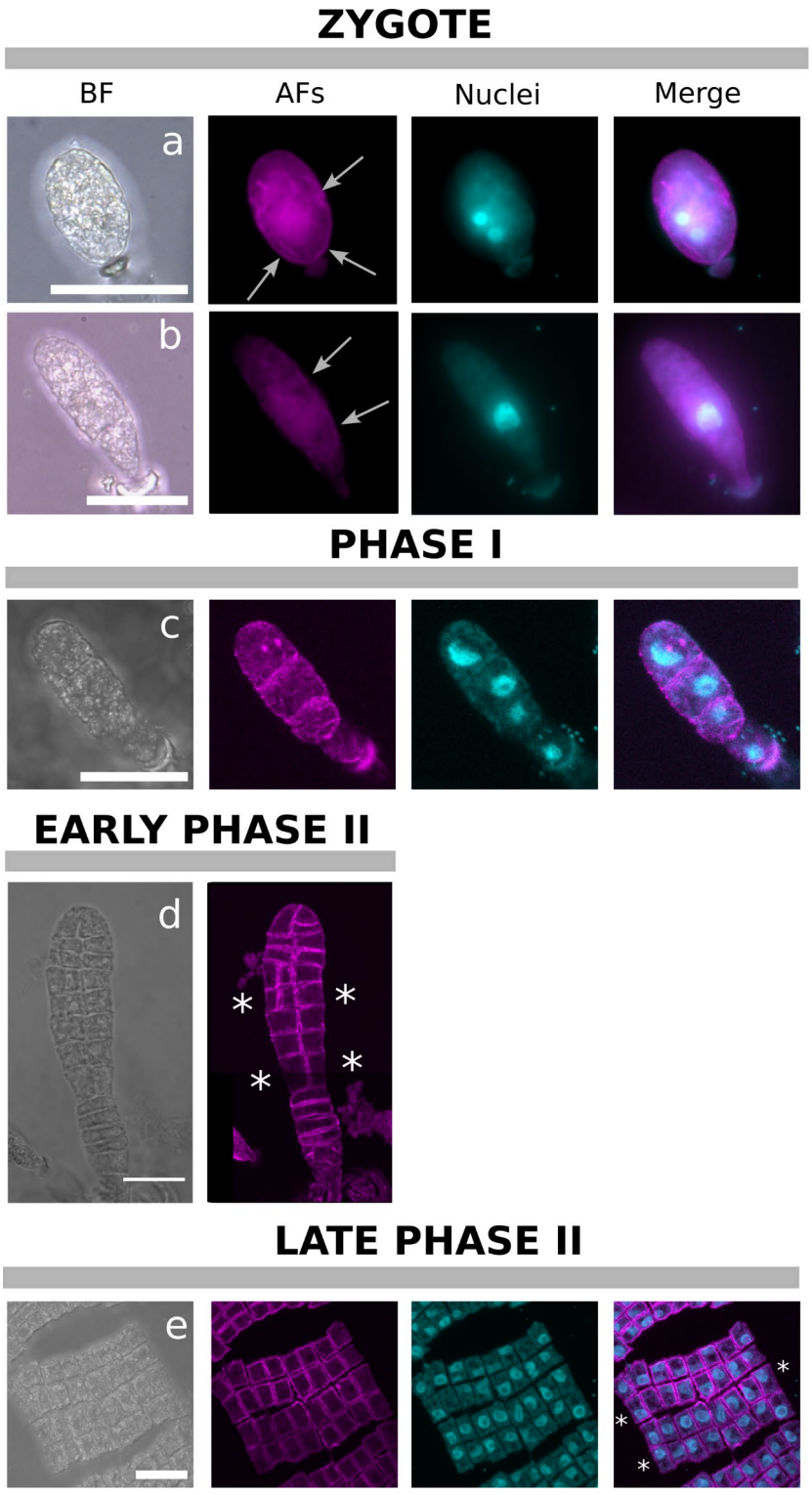

Fig. 3. Actin filament organisation during *Saccharina* embryogenesis. (**a**, **b**): zygotes, (**c**): Phase I embryos, (**d**): early Phase II embryo, (**e**): late Phase II embryo; Magenta column: Actin filaments stained with Alexa Fluor™ 488-phalloidin conjugate (**c**, **e**) or Phalloidin-Rhodamine (**a**, **b**, **d**). Cyan column: Nuclei stained with DAPI; (**a**, **b**): Epifluorescence microscopy; (**c**–**e**): Confocal microscopy. All images are maximal projections of confocal Z-stacks. Grey arrows indicate cortical labelling. White asterisks indicate the weaker signals on the outer edges of the embryo. The images presented have an edited constrast and brightness. Scale bars = 20 µm.

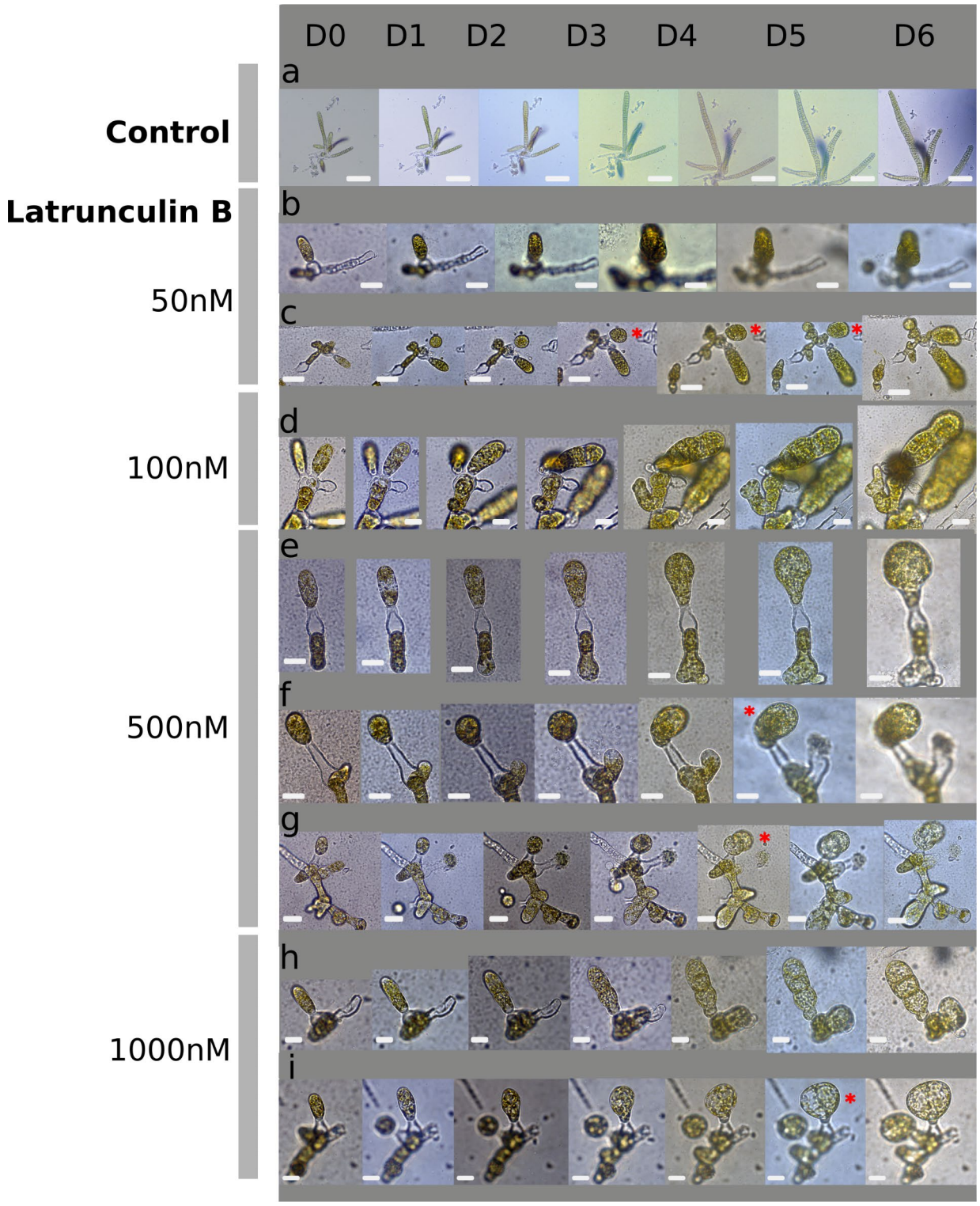

Fig. 4. Morphological response of *Saccharina* zygotes treated with Latrunculin B. Zygotes (D0) were treated with increasing latrunculin B concentrations for 7 days (D0 to D6). A photo is shown for each day for treated zygotes (**b**–**i**) and for DMSO controls (**a**). (**b**, **c**) 50 nM, (**d**) 100 nM, (**e**–**g**): 500 nM; (**h**, **i**): 1 µM. Red asterisks show cell divisions with abnormal orientation. Scale bars = (**a**) 200 µm, (**b**, **c**) 20 µm, (**d**, **i**) 10 µm.

Interestingly, LatB did not affect the localisation of cellulose and sulphated fucans, because these cell wall polysaccharides displayed a similar distribution as that described in control conditions. In the presence of LatB, sulphated fucans still enveloped the zygotes and Phase I and Phase II embryos (Supplementary Fig. S4d), similarly to G-G-rich alginates (Supplementary Fig. S4c). Similarly, cellulose microfibrils were present in the

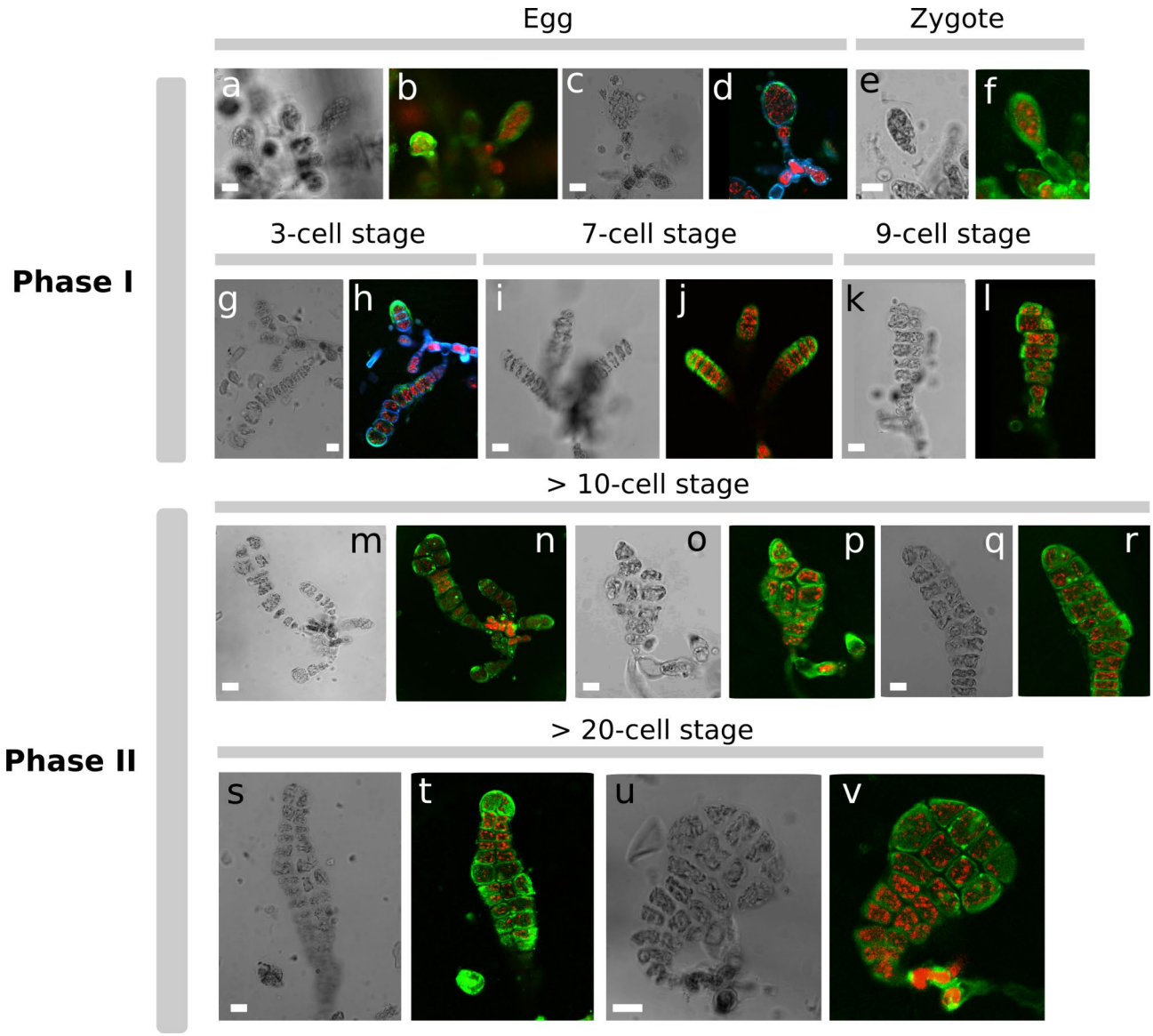

Fig. 5. Labelling of mannuronate-rich alginates in *Saccharina*embryos treated with latrunculin B. Fertilised eggs, zygotes and embryos were labelled with the monoclonal antibody BAM6 after having been treated by 1 µM latrunculin B for 7 days. (**a**, **c**, **e**, **g**, **i**, **k**, **m**, **o**, **q**, **s**, **u**): bright field images. (**b**, **d**, **f**, **h**, **j**, **l**, **n**, **p**, **r**, **t**, **v**): confocal images of FITC-BAM6 labelling (green: FITC; red: chloroplast autofluorescence; blue: Calcofluor white). Scale bars = 10 µm.

external and cross walls in the same manner as in the control conditions (easily observed in Supplementary Fig. S4d for example, Phase I embryos). Therefore, in the early development of *Saccharina* embryo, neither the location of sulphated fucans, nor the formation of cellulose microfibrils seem to depend on AF networks.

Discussion

In this study, we aimed to test whether the assembly of cell wall polysaccharides work in concert with cortical actin filaments to contribute to the dynamics of anisotropic growth of the *Saccharina* embryo, principally during Phase I when the first body plane, namely the apico-basal axis, is established. First, we immunolocalised alginates and fucans in the cell wall of *Saccharina* fertilised eggs, zygotes and embryos. We showed that, in contrast to the other cell wall polysaccharides tested in this study, the accumulation pattern of mannuronate-rich alginates, coincides in space and time with the establishment of the longitudinal axis of the zygote (summarised in Fig. 6, top). We also showed that AFs are necessary for the zygote to establish or maintain this longitudinal axis (Fig. 6, bottom). These results prompt the following question: can mannuronate-rich alginates regulate the formation of the longitudinal axis and, if so, how?

There are many explanations for changes in the immunochemical labelling pattern. This change can be attributed to processes such as epitope degradation, changes in conformation, synthesis or delivery of

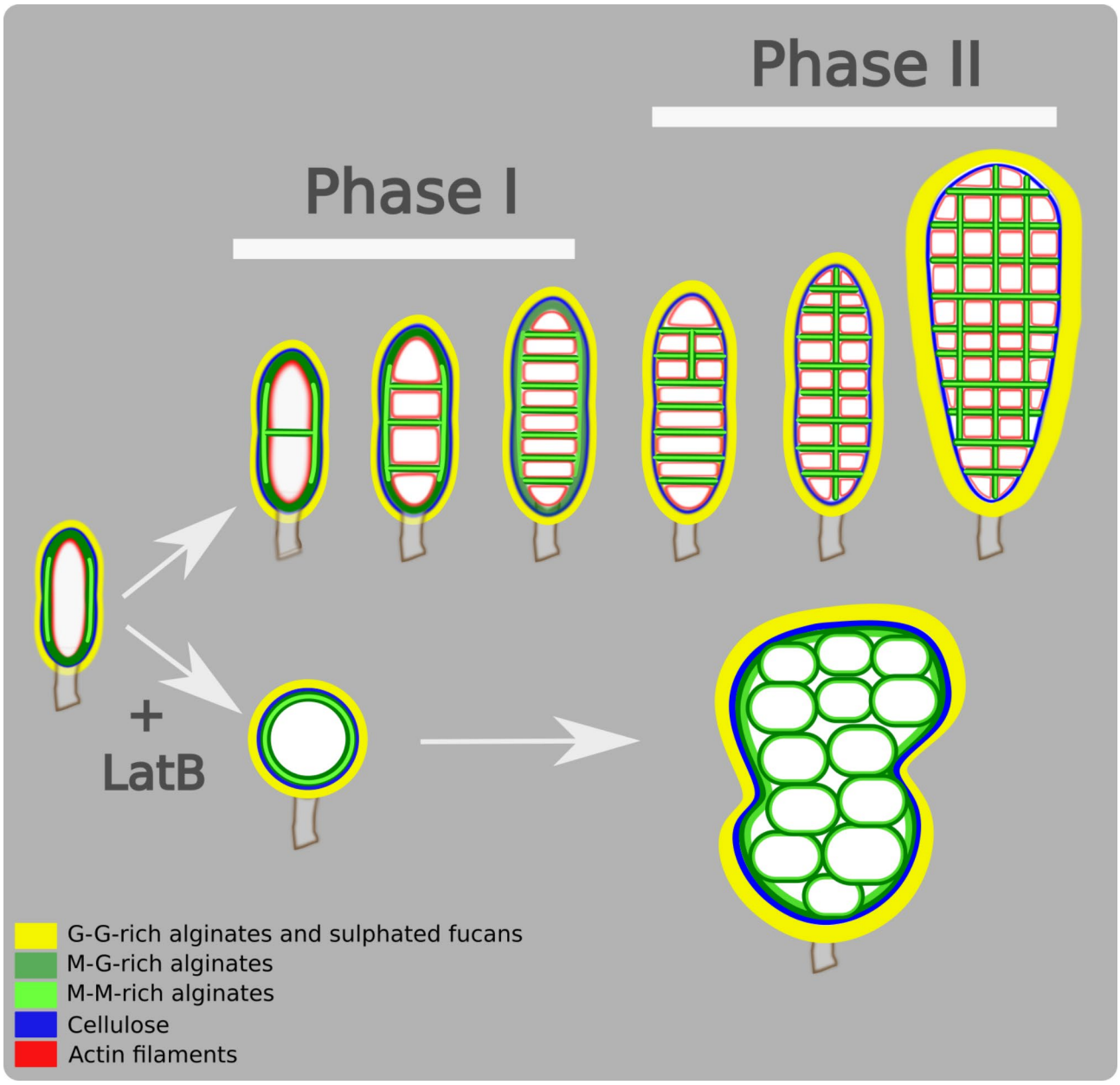

Fig. 6. Summary schematics of the localisation pattern of the cell wall polysaccharides in zygotes and Phase II embryos. Schematics representing the typical body shape and the location of cell wall polysaccharides in the zygote, Phase I and Phase II embryos of *Saccharina latissima*, in standard culture conditions (top) or in the presence of latrunculin B (LatB; bottom). In LatB-treated material, the zygote is spherical and the embryo deformed, made of rounder cells. A layer of mannuronate-rich alginates homogeneously envelops the whole zygote and persists up to late Phase II when the embryo is made of several rows and columns of cells, which may be misaligned. For better clarity, cellulose (in blue) is not represented in the inner cell walls. M, mannuronate residue; G, guluronate residue.

another compound obscuring the targeted epitope[30,31]. Whatever the reasons for the signals appearing and disappearing, our experiments show that polysaccharides fall into two categories based on the spatio-temporal occurrence in the cell walls of the *Saccharina* embryo. The first category, made of guluronate-rich alginates and sulphated fucans, was observed in outer cell walls only (Fig. 6, top, yellow layer). In this compartment, these polysaccharides were homogeneously distributed in the most external layer of the cell wall of the whole embryo. Their localisation pattern did not change from the egg stage to the Phase II embryo. These polysaccharides are a permanent component of the thick, external cell wall enveloping the embryo as of the egg stage and are weakly detected in the more internal, cross walls. Many brown algal embryos synthesise an outer envelope very quickly after fertilisation. In *Saccharina*, the cell wall forms quickly after fertilisation[32]; and our observations). In Fucales, the zygote starts forming a fibrous cell wall less than 5 min after fertilisation (e.g. *Fucus vesiculosus*[33],

which is surrounded by a multilayered cell wall ~ 500 nm thick 4–6 h after fertilisation, and *Pelvetia compressa*[8]). Similarly, in Dictyotales, cell wall secretion is detected within 90 s after fertilisation (e.g. *Dictyota dichotoma*[34]). Thus, our results are consistent with this general pattern.

The second category of cell wall polysaccharides was observed in specific locations, which varied during the growth of the embryo. M-M-rich and M-G-rich alginates were first localised on the surface of the zygote, and then in the transverse and longitudinal cross walls of Phase I and Phase II embryos (summarised in Fig. 6, top, dark and light green layers). Therefore, their spatial pattern changed with time. Furthermore, and very interestingly, M-M-rich alginates were not detected in the apex of zygotes and Phase I embryos, in contrast to M-G-rich alginates. Instead, they formed a corset-like structure on the sides of the zygote and early embryos (up to the 8-cell stage) and, remarkably, this corset-like structure disappeared when the embryo initiated growth along the second body plane: the medio-lateral axis. Upon fertilisation, the egg elongates and preliminary data suggest that the elongation of the *Saccharina* egg is not accompanied by an increase in cell volume. This elongation without enlargement implies that there must be a mechanism to retract the flanks inwards along the Y and Z axes for the egg to increase in length along the longitudinal axis (X-axis). This mechanism has also been described in the zygote of *Dictyota*, which elongates less than 90 s after fertilisation through a mechanism of actomyosin-mediated cell contraction resulting in the modification of cell shape without growth[35]. In addition, in *Saccharina latissima*, longitudinal cell divisions do not occur until the embryo reaches ~ 8 cells, which corresponds to Phase I[13]. Therefore, during Phase I, growth in width is limited in terms of cell expansion and cell division (increase in width = 16.7%) while the embryos double in length (increase of 114.1%). Thus, the corset-like structure of mannuronate-rich alginates, which persists until the 8-cell stage in Phase I embryos, may ensure that cells do not expand laterally by stiffening the cell wall. At the end of Phase I, the corset-like structure disappears and the cells begin to divide longitudinally, allowing the embryo to widen. Knowing whether alginate epimers also accumulate anisotropically along the longitudinal axis of the zygote of *Dictyota*, at the surface of which the cellulose layer seems homogeneously distributed[34], would open the way for comparative studies on the role of mannuronate alginates in the lateral retraction of brown algae zygotes. Furthermore, it is interesting to note that in *Fucus*, M-M-rich alginates accumulate all around the fertilised spherical egg until the signal disappears when the zygote germinates[20]. This ubiquitous location persists in the almost spherical thallus cell of the two-celled *Fucus* embryo, which makes up most of the later embryo, with the most distal region of the rhizoid subsequently degenerating. Therefore, the persistence of an anisotropic pattern of accumulation of M-M-rich alginates may be associated with lateral retraction of the zygote and limiting growth of the embryo in width.

In *Ectocarpus*, the location of alginates along the sporophytic filament does not correlate with cell differentiation, but with the amount of tensile stress at the surface of the cell, which is a combination of turgor, cell curvature and cell wall thickness[36]. Cell areas with lower cell wall thickness and a lower meridional curvature, which are two conditions of high tensile stress[37], have a stronger alginate signature compared with more curved areas with thicker cell walls[36]. Furthermore, when probing the cell surface with atomic force microscopy, spherical cells with lower curvatures displayed a stiffer innermost cell wall layer than cylindrical cells with higher curvatures[36]. In the elongated *Saccharina* zygote, flanks have the lowest meridional and circumferential curvatures. Hence, because the thickness of the external cell wall seems to be similar throughout the egg and embryos (Supplementary Fig. S5), the flanks likely experience the highest tensile stress. In this context, M-M-rich alginates positioned in the flanks of the zygote and embryo may prevent growth in this direction, and thereby promote the establishment of the apico-basal axis in Phase I embryos. In cell-walled organisms, there are several examples of envelopes that surround the embryo and maintain its mechanical balance. In *Arabidopsis*, a recent study reported a transient proteinaceous envelope around early globular-stage embryo[38]. It is thought to control the outward mechanical forces exerted by cell turgor in embryo cells, that escapes the control of the surrounding endosperm, which is deflating at that stage. However, in *Arabidopsis*, and in contrast to *Saccharina*, this control seems to be isotropic, the embryo being almost spherical at that stage.

In addition to the establishment of the embryo longitudinal axis through the retraction of the lateral sides of the fertilised egg, followed by the maintenance of the elongated shape by a corset-like structure of alginates as seen above, the production of cells almost twice as long as they are wide is the second major morphological anisotropy event. Remarkably, these cells are not oriented along the longest axis of the embryo, but perpendicular to it. They are produced by four synchronous cell divisions in the 4-cell stage embryo, parallel to the longest cell axis of their mother cell. The latter is already fairly anisotropic, with an LWR of 1.5. Therefore, these cell divisions diverge from the canonical rules of cell division according to which cells divide along the shortest path, i.e. perpendicularly to the longest cell axis[14,39–41]. In addition, the newly formed transverse cell walls seemed very dense in M-M-rich alginates, judging from the intensity of the signal generated by the BAM6 antibody. Cell divisions parallel to the main stress direction have been reported in plants[42,43], where they are thought to prevent yielding in this direction. Therefore, in the *Saccharina* embryo, cell divisions perpendicular to the longitudinal axis may allow the embryo to better withstand circumferential tensile stress, which — in a prolate ellipsoid — is at its highest at the equatorial plane[44,45].

In summary, at the zygote stage, the alginate corset-like structure may help maintain zygote elongation by preventing widening along the flanks. As the embryo grows, the stress increases and, in response to this stress, the cell division plane is established parallel to the circumferential stress, thereby reinforcing the mechanical resistance of the alginate corset-like structure. As a result, cells are highly anisotropic and incidentally further maintain the apico-basal axis of the embryo during Phase I, especially when the corset-like structure starts to disappear at the end of Phase I.

Although AFs are known to be involved in the formation of the cell wall in brown algae, and especially in the spatial arrangement of cellulose microfibrils[46,47], they have also been shown to be necessary for maintaining the strength of the cell wall[8]. In *Saccharina*, treatment with the AF-depolymerising drug latrunculin B resulted in the loss of anisotropy of the shape of the zygote and the embryo, concomitantly with the loss of the anisotropic

pattern of M-M rich alginate accumulation (summarised in Fig. 6, bottom). This loss of anisotropy strongly suggests a causal relationship between three factors: cortical AFs (1) appear to control, probably together with yet uncharacterised protein complexes, the specific accumulation of M-M-rich alginates (2) along the flanks of the zygote, thereby stiffening the cell wall (3).

Interestingly, in contrast to what was observed in the external cell wall, the presence of mannuronate-rich alginates in the cross walls did not depend on the presence of AFs. AFs are necessary for cytokinesis of brown algal cells[,19,48,49] and in our experiment, the cells labelled in Phase II *Saccharina* embryos had already divided. Therefore, LatB-mediated depolymerisation of AFs would mainly affect the maintenance of the organisation of the previously formed cell wall. Although the signal corresponding to mannuronate-rich alginates seemed diffuse, potentially revealing some disorganisation of the cell wall, the signal remained homogeneously distributed at the surface of all cross walls. This diffuse pattern of distribution suggests that the maintenance of M-M-rich alginates in cross walls and external cell walls is controlled by different mechanisms. Nevertheless, the AFs organised mainly parallel to the Z-axis shows a potential relationship between AFs and mechanical feedback, reminiscent of cortical microtubules in plants[50,51].

In addition to the cortical AFs that control the formation of the corset-like structure, we have recently shown that the development of the longitudinal axis of the embryo depends on the connection with the maternal tissue. The integrity of the stalk, a structure corresponding to the remnant oogonium wall, is necessary for the zygote and embryo to develop the apico-basal axis[15]. A signal diffusing from the stalk through the basal cell of the embryo appears to inhibit longitudinal divisions in the embryo[16]. Upon embryo growth, the apical cells at a distance of at least 40 µm from the stalk can engage in longitudinal division. Beyond identifying the nature of this signal, the question of whether it controls the organisation of cortical AFs and the spatial pattern of M-M-rich alginates is the next important step in continuing to determine the mechanisms and signalling pathways that control *Sacharrina* embryogenesis. Before undertaking this endeavour, or perhaps concomitantly, it is necessary to confirm the role of this alginate corset-like structure in the elongation of the zygote, and thus in the establishment of the apico-basal axis of *Saccharina* embryo. Treatment with enzymes degrading the cell wall of brown algae, such as alginate lyases, results in a massive boost of bacterial contamination at the surface of the alga, due to the release of small glycans or monosaccharides in the medium. Therefore, a mechanical approach, or mutants with a reduced M-M-rich alginate composition are more promising to weaken the corset-like structure and test its effect on the shape anisotropy of the zygote and young embryo. However, as we have observed in this study, M-M-rich alginates are found mainly in the innermost layers of the external and cross cell walls, like M-G-rich alginates, and unlike G-G-rich alginates which are generally found in the outermost layers. Similar observations have been reported in *Ectocarpus*[52] and anticipated in *Fucus*[53]. This location suggests that mannuronates are delivered to the plasma membrane before being transformed into guluronates by the mannuronate C5-epimerases[54] present in the cell walls[19]. Alternatively, mannuronate-rich alginates may be degraded by alginate lyases recently identified in brown algae[19,55]. These two hypotheses could explain the disappearance of the M-M-rich alginate corset-like structure at the end of Phase I, but on the whole they rule out the possibility of making an embryo without an M-M-rich alginate corset-like structure: first, M-M-rich alginates belong to the same cell wall layer as M-G alginates, which makes them difficult to destroy specifically, for example by laser irradiation; second, mutants lacking mannuronates will also lack guluronates, which will be highly detrimental to the alga, if not lethal.

In conclusion, here we established a functional relationship between the anisotropic growth of the embryo of *Saccharina latissima*, and the presence of a corset-like structure of mannuronate-rich alginates in the zygote, through the presence of cortical actin filaments. When AFs are depolymerised, the level of embryo anisotropy decreases and the corset-like structure disappears, replaced by an alginate layer homogeneously enveloping the zygote and embryo. This raises many questions, such as how cortical AFs located homogeneously around the zygote can control the formation of a corset-like structure only along the flanks of the embryo, how mannuronate alginates organised as a corset-like structure control the widening of the zygote and embryo, whereas they are organised as a layer distributed homogeneously in isotropic zygotes, which will need to be resolved by future work.

Materials and methods

Preparation of *Saccharina* embryos

Embryos were produced from fertilisation of female gametophytes as described in[56] and distributed in dishes with glass bottom (NEST). Briefly, gametogenesis was induced under white light conditions at 16 µmol photons m^{-2} s^{-1}, 14:10 light: dark photoperiod and 13 °C and full Provasoli enriched seawater (PES)[56,57]. Then, the embryos were exposed to more intense white light (40 µmol photons m^{-2} s^{-1}) to promote embryo growth.

Embryo and cell morphometry.

Data for embryo and cell morphometrics were taken from three sources: measurements of zygote dimensions ($n = 15$) and previous measurements of control embryos ($n = 10$) at stages ≥ 2-cells, published in[15,16]. Zygote dimensions were measured on microscopic images using Fiji[58], and dimensions of embryos and their cells were computed by the software described in[16]. For the embryo and cell measurements, the sliding window mean and the lowess function were computed using Python 3[59].

BAM immunolabelling

We looked for antibodies able to display anisotropic mapping of cell wall polysaccharides. BAM antibodies[20,21] recognise polysaccharide blocks that are more or less abundant in mannuronate (M) or guluronate (G). They are therefore not, and in particular the BAM6-11 series, strictly specific to a given homogeneous polysaccharide, but rather allow a relative assessment of the overall composition of cell wall polysaccharides. BAM antibodies were obtained from SeaProbes (Roscoff, France). Immunolocalisation protocol was adapted from[36]. Briefly,

embryos were fixed with 4% paraformaldehyde dissolved in H_2O: sea water (NSW hereafter) (50:50) for 70 min at room temperature. These fixation conditions prevented cell shrinkage, as the half-concentration of seawater maintained cell turgor during the fixation step. Cells were then washed once with NSW: PBS (50:50), twice with PBS for 10 min and blocked in PBS with 5% milk for 1 h at room temperature. The embryos were incubated overnight at 4 °C with the BAM monoclonal primary antibodies[20,21] diluted 1:10 in PBS with 5% milk. Antibodies were washed with PBS three times for 5 min. The cells were then incubated overnight at 4 °C with the secondary antibody anti-rat conjugated with FITC diluted 1:100 in PBS. Antibodies were washed three times for 10 min with PBS. The embryos were then stained for 30 min with 20 µM Calcofluor (Fluorescent Brightener 28, Sigma-Aldrich,St. Louis, MI, USA) and washed three times with PBS. Finally, the embryos were mounted in Vectashield (H-1000-10 (Vector®, with or without DAPI) and covered with a coverslip. Each labelling was repeated at least 3 times.

Labelling actin filaments

The actin labelling protocol was optimised based on[60]. Firstly, the material was incubated for 30 min in prefix solution containing 300 µM m-maleimido benzoic acid N-hydroxy succinimide ester (MBS; Sigma-Aldrich®), 0.2% Triton X-100 and 2% dimethyl sulphoxide (DMSO) in microtubule-stabilising buffer (MTB, 50 mM PIPES, 5 mM ethyleneglycol bis (aminoethyl ether)-tetraacetic acid (EGTA), 5 mM $MgSO_4.7H_2O$, 25 mM KCl, 4% NaCl, 2.5% polyvinylpyrrolidone 25 (PVP), 1 mM DL-dithiothreitol (DTT), pH7.4), in the dark and at room temperature. Fixation followed without washes, changing the medium to 2% PFA, 0.2% glutaraldehyde (GTA) and 2 U of rhodamine-conjugated phalloidin (Ph-Rh; R415, Invitrogen™) or Alexa Fluor™ 488-conjugated phalloidin (Ph-Alexa488; A12379, Invitrogen™) in MTB for 1.5 h, in the dark and at room temperature. Then the embryo tissue was washed with 1:1 MTB: PBS, and incubated in cell wall lysis buffer (2% w/v Cellulase Onozuka R-10 (Yakult Pharmaceutical industry Co., Ltd.), 2% w/v hemicellulase (Sigma-Aldrich®), 1% driselase (Sigma-Aldrich®), 1.5% macerozyme R-10 (Yakult Pharmaceutical industry Co., Ltd.), 50 U/ml alginate lyase-G (M. Czjzek and M. Jam, Laboratory of Integrative Biology of Marine Models, Station Biologique de Roscoff), 5 U Ph-Rh/ Ph-Alexa488 and 0.15% Triton X-100 in 1:1 MTB: PBS) for 10 min, in the dark and at room temperature. An extraction step followed a short series of washes. The tissues were incubated for 10 min in extraction solution (5% DMSO, 3% Triton X-100 and one of the phalloidin conjugates (2U) in PBS) in the dark and at room temperature. After washing with 1:1 MTB: PBS, the tissue was treated with the phallodin stain (15 U of the chosen phalloidin conjugate in 1:1 MTB: PBS) overnight at 4 °C in the dark. After washing, the nuclei were stained with DAPI. Vectashield H-1000-10 (Vector®) was used for mounting the samples.

The orientation of AFs was measured with the batch mode of FibrilTool included in the MT_Angle2Ablation workflow (https://github.com/VergerLab/FibrilTool_Batch_Workflow[61]). The apico-basal axis of the embryo was set as reference (angle = 0). The angles were processed with basic statistics in R.

Latrunculin B treatments

Egg, zygotes and embryos of 2 to 8 cells were treated with a range of concentrations from 50 nM to 1 µM of latrunculin B (Sigma Aldrich) or incubated in 0.1% or 1% DMSO (LatB solvant used as a control) for one week. Their growth was then monitored every day for up to 7 days under a bright field microscope (DMI8 inverted microscope, Leica Microsystems). Samples treated for 1 week with 1 µM LatB were used for the immunostaining experiments (results shown in Supplementary Fig. S2).

Image acquisition

Image data were acquired with a bright field and epifluorescence microscope DMI8 (Leica Microsystems) equipped with the colour camera DMC4500 (Leica Microsystems), Leica EL6000 compact light source and controlled with LAS X v3.0 (Leica Microsystems), and TCS SP5 AOBS inverted confocal microscope (Leica Microsystems) controlled by the LASAF v2.2.1 software (Leica Microsystems), with the objective HCX PL APO CS 20.0 × 0.70 DRY UV. The wavelengths of excitation of DAPI/Calcofluor white, FITC and chloroplasts were respectively 405 nm, 488 nm and 496 nm. The emission wavelength ranges were respectively 415–485 nm, 551–620 nm and 668–765 nm. The opening of the pinhole was 1AU. Line average and line accumulation were set to 1. Observation of rhodamine or Alexa Fluor™ 488-phalloidin-labelled AFs was carried out using a TCS SP8 AOBS inverted confocal microscope (Leica Microsystems) with a 100X/N.A 1.4 objective. The data were analysed using Fiji[58].

Transmission electronic microscopy

Live embryos were left to grow for up to 6 days under white light, then fixed with 1% glutaraldehyde and 1% paraformaldehyde (both from Sigma-Aldrich) in sterile, 0.2 µm-filtered seawater for 2 h at 13 °C. Then, the fixation medium was gradually changed to 0.1 M sodium cacodylate. Post-fixation consisted of incubating the thalli in 1% OsO_4 in 0.1 M sodium cacodylate at 4 °C overnight. Following washes with 0.1 M sodium cacodylate, the embryos were dehydrated using an ethanol: sodium cacodylate gradient. For infiltration, Spurr resin gradually replaced ethanol (Spurr, 1969), with fresh resin for the final step before polymerisation. Ultra-thin Sects. (50–70 nm) from the embedded embryos were mounted on copper grids (Formvar 400 mesh; Electron Microscopy Science©) and stained with 2% uranyl acetate for 10 min (Woods and Stirling, 2013) and 2% lead citrate for 3 min at room temperature (Reynolds, 1963). Sections were observed using a JEM-1400 Flash TEM microscope (JEOL Ltd.).

Data availability

All data are available as Supplementary Information files.

Received: 29 July 2024; Accepted: 17 December 2024
Published online: 07 January 2025

References

1. Charrier, B., Le Bail, A. & de Reviers, B. Plant proteus: Brown algal morphological plasticity and underlying developmental mechanisms. *Trends Plant Sci.* **17**, 468–477 (2012).
2. Charrier, B. et al. Development and physiology of the brown alga *Ectocarpus siliculosus*: Two centuries of research. *New. Phytol.* **177**, 319–332 (2008).
3. Le Bail, A. et al. Initial pattern of development of the brown alga *Ectocarpus siliculosus* (Ectocarpales, Phaeophyceae) sporophyte. *J. Phycol.* **44**, 1269–1281 (2008).
4. Theodorou, I. & Charrier, B. Brown Algae: Ectocarpus and Saccharina as experimental models for developmental biology. In *Handbook of Marine Model Organisms in Experimental Biology* 27–47 (CRC, 2021).
5. Nehr, Z. et al. Tip growth in the brown alga *Ectocarpus* is controlled by a RHO-GAP-BAR domain protein independently from F-actin organisation. bioRxiv 2021.08.28.458042. https://doi.org/10.1101/2021.08.28.458042 (2021).
6. Berger, F. & Brownlee, C. Photopolarization of the *Fucus* sp. zygote by blue light involves a plasma membrane redox chain. *Plant Physiol.* **105**, 519–527 (1994).
7. Hable, W. E. & Kropf, D. L. Sperm entry induces polarity in fucoid zygotes. *Development* **127**, 493–501 (2000).
8. Bisgrove, S. R. & Kropf, D. L. Cell wall deposition during morphogenesis in fucoid algae. *Planta* **212**, 648–658 (2001).
9. Hable, W. E., Miller, N. R. & Kropf, D. L. Polarity establishment requires dynamic actin in fucoid zygotes. *Protoplasma* **221**, 193–204 (2003).
10. Goodner, B., Quatrano, R. Fucus embryogenesis: A model to study the establishment of polarity. *Plant Cell* **5**, 1471–1481 (1993).
11. Kanda, T. On the gametophytes of some Japanese species of Laminariales III. *Sci. Papers Inst. Algol. Res. Fac. Sci. Hokkaido Imperial Univ.* **2**, 155–193 (1941).
12. Sauvageau, C. Recherches sur les laminaires des cotes de France. *Mem. Acad. Sci.* **56**, 1–240 (1918).
13. Theodorou, I. & Charrier, B. The shift to 3D growth during embryogenesis of kelp species, atlas of cell division and differentiation of *Saccharina Latissima*. *Development* **150**, dev201519 (2023).
14. Errera, L. Über Zellformen und Siefenblasen. *Bot. Centralblatt* **34**, 395–399 (1888).
15. Boscq, S., Billoud, B. & Charrier, B. Cell-autonomous and non-cell-autonomous mechanisms concomitantly regulate the early developmental pattern in the kelp *Saccharina latissima* embryo. *Plants* **13**, 1341 (2024).
16 Boscq S et al. MUM, a maternal unknown message, inhibits early establishment of the medio-lateral axis in the embryo of the kelp *Saccharina latissima*. *Development* **151**, dev202732 (2024).
17. Charrier, B., Rabillé, H. & Billoud, B. Gazing at cell wall expansion under a golden light. *Trends Plant. Sci.* **24**, 130–141 (2019).
18. Deniaud-Bouët, E., Hardouin, K., Potin, P., Kloareg, B. & Hervé, C. A review about brown algal cell walls and fucose-containing sulfated polysaccharides: Cell wall context, biomedical properties and key research challenges. *Carbohydr. Polym.* **175**, 395–408 (2017).
19. Mazéas, L. et al. Assembly and synthesis of the extracellular matrix in brown algae. In *Seminars in Cell & Developmental Biology* S1084-9521(22)00071–4 https://doi.org/10.1016/j.semcdb.2022.03.005 (2022).
20. Torode, T. A. et al. Dynamics of cell wall assembly during early embryogenesis in the brown alga *Fucus*. *J. Exp. Bot.* **67**, 6089–6100 (2016).
21. Torode, T. A. et al. Monoclonal antibodies directed to fucoidan preparations from brown algae. *PLoS ONE* **10**, e0118366 (2015).
22. Yonamine, R. et al. Changes in cell wall structure during rhizoid formation of *Silvetia babingtonii* (Fucales, Phaeophyceae) zygotes. *J. Phycol.* **57**, 1356–1367 (2021).
23. Popper, Z. A. et al. volution and diversity of plant cell walls: From algae to flowering plants. *Annu. Rev. Plant Biol.* **62**, 567–590 (2011).
24. Hable, W. E. & Kropf, D. L. The Arp2/3 complex nucleates actin arrays during zygote polarity establishment and growth. *Cell Motil.* **61**, 9–20 (2005).
25. Hable, W. E., Reddy, S. & Julien, L. The Rac1 inhibitor, NSC23766, depolarizes adhesive secretion, endomembrane cycling, and tip growth in the fucoid alga, Silvetia compressa. *Planta* **227**, 991–1000 (2008).
26. Henry, C. A., Jordan, J. R. & Kropf, D. L. Localized membrane-wall adhesions in*Pelvetia* zygotes. *Protoplasma* **190**, 39–52 (1996).
27. Katsaros, C., Karyophyllis, D. & Galatis, B. F-actin cytoskeleton and cell wall morphogenesis in brown algae. *Cell Biol. Int.* **27**, 209–210 (2003).
28. Katsaros, C., Karyophyllis, D. & Galatis, B. Cytoskeleton and morphogenesis in brown algae. *Ann. Bot.* **97**, 679–693 (2006).
29. Wakatsuki, T., Schwab, B., Thompson, N. C. & Elson, E. L. Effects of cytochalasin D and latrunculin B on mechanical properties of cells. *J. Cell Sci.* **114**, 1025–1036 (2001).
30. Hawes, D. et al. Immunohistochemistry *Mod. Surg. Pathol.* 48–70. https://doi.org/10.1016/B978-1-4160-3966-2.00016-3 (2009).
31. Vázquez-Gutiérrez, J. L. & Langton, M. Current potential and limitations of immunolabeling in cereal grain research. *Trends Food Sci. Technol.* **41**, 105–117 (2015).
32. Motomura, T. Ultrastructure of fertilization in *Laminaria angustata* (Phaeophyta, Laminariales) with emphasis on the behavior of centrioles, mitochondria and chloroplasts of the sperm. *J. Phycol.* **26**, 80–89 (1990).
33. Pollock, E. G. Fertilization in *Fucus*. *Planta* **92**, 85–99 (1970).
34. Bogaert, K. A., Beeckman, T. & De Clerck, O. Egg activation-triggered shape change in the Dictyota dichotoma (Phaeophyceae) zygote is actin–myosin and secretion dependent. *Ann. Bot.* **120**, 529–538 (2017).
35. Bogaert, K. A., Beeckman, T. & De Clerck, O. Two-step cell polarization in algal zygotes. *Nat. Plants* **3**, 16221 (2017).
36. Rabillé, H. et al. Alginates along the filament of the brown alga Ectocarpus help cells cope with stress. *Sci. Rep.* **9**, 12956 (2019).
37. Lockhart, J. A. An analysis of irreversible plant cell elongation. *J. Theor. Biol.* **8**, 264–275 (1965).
38. Harnvanichvech, Y. et al. An elastic proteinaceous envelope encapsulates the early *Arabidopsis* embryo. *Development* **201943** https://doi.org/10.1242/dev.201943 (2023).
39. Besson, S. & Dumais, J. Universal rule for the symmetric division of plant cells. *Proc. Natl. Acad. Sci.* **108**, 6294–6299 (2011).
40. Besson, S. & Dumais, J. Stochasticity in the symmetric division of plant cells: when the exceptions are the rule. *Front. Plant. Sci.* **5**, (2014).
41. Hofmeister, W. Zusatze und Berichtigungen zu den 1851 veroffentlichen Untersuchungen der Entwicklung hoherer Kryptogamen. *Jahrb Wiss Bot.* **3**, 259–193 (1863).
42. Louveaux, M., Julien, J. D., Mirabet, V., Boudaoud, A. & Hamant, O. Cell division plane orientation based on tensile stress in *Arabidopsis thaliana*. *Proc. Natl. Acad. Sci. U.S.A.* **113**, E4294–E4303 (2016).
43. Rasmussen, C. G. & Bellinger, M. An overview of plant division-plane orientation. *New Phytol.* **219**, 505–512 (2018).
44. Hejnowicz, Z., Heinemann, B. & Sievers, A. Tip growth: Patterns of growth rate and stress in the *Chara* rhizoid. *Z. Pflanzenphysiol.* **81**, 409–424 (1977).
45. Rabillé, H. et al. The brown algal mode of tip growth: Keeping stress under control. *PLoS Biol.* **17**, e2005258 (2019).
46. Karyophyllis, D., Katsaros, C., Dimitriadis, I. & Galatis, B. F-actin organization during the cell cycle of *Sphacelaria rigidula* (Phaeophyceae). *Eur. J. Phycol.* **35**, 25–33 (2000).

47. Katsaros, C. I., Karyophyllis, D. A. & Galatis, B. D. Cortical F-actin underlies cellulose microfibril patterning in brown algal cells. *Phycologia* **41**, 178–183 (2002).
48. Katsaros, C., Nagasato, C., Terauchi, M. & Motomura, T. Cytokinesis in brown algae. In *Advances in Algal Cell Biology* (eds Gruyter, D.) 224 (Berlin, 2013).
49. Nagasato, C. et al. Membrane fusion process and assembly of cell wall during cytokinesis in the brown alga, *Silvetia babingtonii* (Fucales, Phaeophyceae). *Planta* **232**, 287–298 (2010).
50. Hamant, O., Inoue, D., Bouchez, D., Dumais, J. & Mjolsness, E. Are microtubules tension sensors? *Nat. Commun.* **10**, 2360 (2019).
51. Zhao, F. et al. Microtubule-mediated Wall Anisotropy contributes to Leaf Blade Flattening. *Curr. Biol.* **30**, 3972–3985e6 (2020).
52. Terauchi, M., Nagasato, C., Inoue, A., Ito, T. & Motomura, T. Distribution of alginate and cellulose and regulatory role of calcium in the cell wall of the brown alga *Ectocarpus siliculosus* (Ectocarpales, Phaeophyceae). *Planta* **244**, 361–377 (2016).
53. McCully, M. E. A note on the structure of the cell walls of the brown alga *Fucus*. *Can. J. Bot.* **43**, 1001–1004 (1965).
54. Fischl, R. et al. The cell wall active mannuronan C5-epimerases in the model brown alga *Ectocarpus*: From gene context to recombinant protein. *Glycobiology* https://doi.org/10.1093/glycob/cww040 (2016).
55. Inoue, A. & Ojima, T. Functional identification of alginate lyase from the brown alga *Saccharina japonica Sci. Rep.* **9**, 4937 (2019).
56. Theodorou, I., Opsahl-Sorteberg, H. G. & Charrier, B. Preparation of zygotes and embryos of the kelp *Saccharina latissima* for cell biology approaches. *Bio-protocol* e4132–e4132 (2021).
57. Le Bail, A. & Charrier, B. Culture methods and mutant generation in the filamentous brown algae *Ectocarpus siliculosus*. In *Plant Organogenesis*, Vol. 959 (eds De Smet, I.) 323–332 (Humana, 2013).
58. Schindelin, J. et al. Fiji—An open source platform for biological image analysis. *Nat. Methods* **9**, 676–682 (2012).
59. Van Rossum, G. & Drake, F. L. The Python Language Reference, Release 3.11.5, Python Software Foundation (2023).
60. Rabillé, H., Koutalianou, M., Charrier, B. & Katsaros, C. Actin fluorescent staining in the filamentous brown alga *Ectocarpus siliculosus*. In *Protocols for Macroalgae Research*, Vol. 1 (eds Charrier, B., Wichard, T. & Reddy, C.) 365–379 (Taylor & Francis group, CRC, 2018).
61. Boudaoud, A. et al. FibrilTool, an ImageJ plug-in to quantify fibrillar structures in raw microscopy images. *Nat. Protoc.* **9**, 457–463 (2014).

Acknowledgements

S.B. was funded by the Bretagne Regional Council ("PRIMAXIS" project, grant number 1749) and Sorbonne University. I.T. was funded by an ARED grant from the Bretagne Regional Council ("PUZZLE" project) and NMBU. We are grateful to MITI CNRS for additional financial support and to Sophie Le Panse (Merimage platform, Roscoff Biological Station), for the TEM experiments. Part of the work was funded by the European Union (ERC, ALTER e-GROW, project number 101055148). Views and opinions expressed are those of the author(s) only and do not necessarily reflect those of the European Union or the European Research Council Executive Agency. Neither the European Union nor the granting authority can be held responsible for them. For purposes of open access dissemination, the authors applied for a CC BY-NC license for this document.

Author contributions

S.B., I.T, R.M, A.L-B and S.C. performed the experiments. S.B, I.T , A.L-B , B.B and B.C prepared the figures. B.B. prepared the table. B.C wrote the main manuscript text. All authors reviewed the manuscript."

Declarations

Competing interests

The authors declare no competing interests.

Additional information

Supplementary Information The online version contains supplementary material available at https://doi.org/10.1038/s41598-024-83814-5.

Correspondence and requests for materials should be addressed to B.C.

Reprints and permissions information is available at www.nature.com/reprints.

Publisher's note Springer Nature remains neutral with regard to jurisdictional claims in published maps and institutional affiliations.